INTERNATIONAL JOURNAL FOR NUMERICAL AND ANALYTICAL METHODS IN GEOMECHANICS, VOL. 10, 177–190 (1986)

DYNAMIC STABILITY ANALYSIS OF UNDRAINED SIMPLE SHEAR ON WATER-SATURATED GRANULAR SOILS

I. VARDOULAKIS

Department of Civil and Mineral Engineering, University of Minnesota, Minneapolis, MN 55455, U.S.A.

SUMMARY

Dynamic stability of undrained, simple-shear deformations on water-saturated granular soil specimens is discussed. The soil is described by a 2D-flow theory of plasticity for frictional and dilatant material. Contractant material becomes unstable (liquefies) at the state of maximum shear stress, whereas dilatant material becomes unstable after the state of maximum effective stress obliquity is reached in the softening regime of the background drained behaviour. In both cases the correct evolution equations for the growth coefficient of the instability are derived and compared with the results of the inertia-free formulation of the problem.

INTRODUCTION

In recent years numerous and extensive studies on liquefaction phenomena in water-saturated granular soils have appeared in the literature.[1] The majority of the existing experimental studies on liquefaction concentrate on measuring stresses, strains and pore-pressure build-up in undrained tests on specimens subject to monotonous or cyclic loading histories.[2,3] Following these observations, several sophisticated constitutive models have been suggested, which more or less accurately predict pore-pressure build-up during undrained deformations.[4] In both types of loading, liquefaction is perceived to occur as soon as the effective stress path touches the failure envelope.

A quite different approach consists of trying to describe liquefaction as a result of mechanical instability. This approach was originally suggested in a paper by Rice,[5] where the stability of pore-pressure generation during undrained shear of a long, dilatant rock layer was investigated (Figure 1). Rice's approach is based on a simple elastic-plastic constitutive model for a material with friction and dilatancy.[6,7] For a monotonous increase of the shear stress, τ, and for constant normal stress, σ, the state of effective stresses, σ'_{ij}, and the excess pore-water pressure, p, during undrained shear are computed. At any given state of the deformation the question of stability of the pore-pressure generation is asked. This is done by considering a small perturbation Δp of the current pore-pressure and by looking for its evolution in time under constant boundary stresses. This formulation yields a consolidation-type equation for Δp:

$$\frac{\partial^2 \Delta p}{\partial x_2^2} = c \frac{\partial \Delta p}{\partial t} \tag{1}$$

where x_2 is the co-ordinate normal to the layer and t is time. The diffusivity coefficient, c, in equation (1) is a function of the state variables which appear in the assumed constitutive model.

0363–9061/86/020177–14$07.00

Received 21 June 1984
Revised 11 March 1985

Solutions of equation (1) evolve in time as $\exp(ft)$, where

$$f = -\left[\frac{(2m+1)\pi}{l}\right]^2 \frac{1}{c}, \quad m = 1, 2, \ldots \tag{2}$$

is usually called the growth coefficient. Stable configurations are perceived to be those with $c > 0$, because in that case any perturbation Δp of the pore-pressure will fade as time elapses. On the other hand, a state with $c < 0$ is unstable because perturbations of the pore-pressure are exponentially amplified.

Rice[5] observed that the growth coefficient f (or according to equation (2) the quantity $1/c$) is proportional to the tangent modulus, h, of the effective stress-ratio–strain curve describing the background drained material behaviour. Consequently, undrained shear of dilatant frictional material becomes unstable as soon as the material, in terms of effective stress ratio, starts to strain-soften. This means that any state beyond the state S_C (C for Coulomb) of maximum effective stress-ratio is unstable. For a dilatant material the evolution of the growth coefficient, f, is regular, increasing as the tangent modulus $(-h)$.

It will be shown here that for contractant material c changes sign at the state S_T (T for Tresca) of maximum shear stress, and that is evolves as $(h - h_T)$, where $h_T > 0$ is the value of the hardening modulus at S_T. In this case the evolution of the growth coefficient is anomalous, since at S_T f is switching from $-\infty$ to $+\infty$ and for states following $S_T f$ is decreasing.[8] This anomaly is pointing to an error which might arise from applying Rice's inertia-free formulation in the case of contractant material. In studying slow diffusion processes the assumption is usually made that inertial effects are negligible as compared to dissipative effects, and thus second order time derivatives of the various quantities are neglected. Since $|c| \ll 1$ in the vicinity of S_T this assumption cannot be made, because for sufficiently small values of c, inertial effects should become important.

As far as soils are concerned, medium dense samples undergo a stable dilatant hardening process, for the soil presumably never reaches the limit condition.[2,3] On the other hand, Vaid and Chern[3] remark that for monotonic, undrained triaxial compression tests on loose sand samples 'the deviator stress and the porewater pressure increased progressively with very small overall strain development and the effective stress path [was] moving towards the failure envelope. This trend continued until a state of stress was reached at which the sample became unstable. A sudden decrease in deviator occurred accompanied by a sharp increase in porewater pressure and axial strain in a very short period of time. This flow deformation... was stopped by dilation once the sample developed sufficient strain...'. These experimental observations strongly suggest that the above outlined inertia-free formulation is not describing correctly the evolution of the pore pressures during the unstable phase of the deformation, which is usually called the phase of flow deformation.

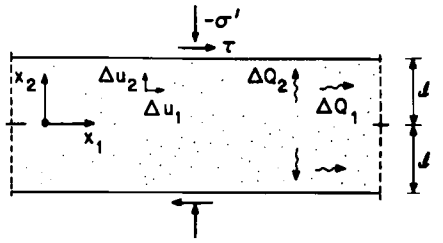

Figure 1. Infinitely long layer under normal and shear stress

In this paper, the dynamic stability analysis of undrained simple shear is presented. The analysis is restricted to the study of the incipient part of the flow deformation phase. First, the constitutive equations of the 2D-flow theory of plasticity for frictional and dilatant material are outlined and applied in order to describe in terms of effective stresses the stress–strain behaviour of a granular soil subjected to undrained simple shear. Stability of undrained shear is treated within an inertia-free and a dynamic formulation of a perturbation problem. Eigenvalue equations are formulated and solved numerically. Finally, asymptotic expressions for the evolution law of the growth coefficient of the instability are derived and are compared with expressions derived from the inertia-free formulation.

2D-FLOW THEORY OF PLASTICITY

Let $\sigma_{ij}(\Delta\sigma_{ij})$ denote the total Cauchy stress (increment) and let p (Δp) denote the pore-water pressure (increment). According to Terzaghi's effective stress principle, constitutive equations are expressed in terms of the effective stress $\sigma'_{ij}(\Delta\sigma'_{ij})$ defined through the following stress decomposition:

$$\sigma_{ij} = \sigma'_{ij} - p\delta_{ij} \quad (p > 0) \tag{3}$$

As presented in a previous publication,[8] the constitutive equations of the simplest 2D-flow theory of plasticity for frictional and dilatant material under fully loading conditions are

$$\begin{aligned} \Delta e_{ij} &= \frac{1}{2G}\Delta s_{ij} + \frac{1}{2p'h}\left(\frac{\Delta\tau}{\tau} - \frac{\Delta p'}{p'}\right)s_{ij} \\ \Delta\varepsilon &= -\frac{1}{K}\Delta p' + \frac{\mu\beta}{h}\left(\frac{\Delta\tau}{\tau} - \frac{\Delta p'}{p'}\right) \end{aligned} \tag{4}$$

where $s_{ij}(\Delta s_{ij})$ and $p'(\Delta p')$ are the deviator of the effective stress and the effective pressure, respectively:

$$\sigma'_{ij} = s_{ij} - p'\delta_{ij} \quad (p' > 0) \tag{5}$$

and Δe_{ij} and $\Delta\varepsilon$ are the total deviatoric strain increment and volumetric strain increment, respectively:

$$\Delta\varepsilon_{ij} = \Delta e_{ij} + \tfrac{1}{2}\Delta\varepsilon\delta_{ij} \tag{6}$$

In equations (4) τ is the shear stress intensity, defined as

$$\tau = (\tfrac{1}{2}s_{ij}s_{ji})^{1/2} \tag{7}$$

K and G are the elastic compression and shear moduli of the soil skeleton, related to the Poisson's ratio ν through

$$\alpha = \frac{K}{G} = \frac{1}{1-2\nu} \tag{8}$$

μ and β are appropriate friction and dilatancy functions of the porosity, n, and of the accumulated plastic shear strain:

$$\gamma^p = \int \Delta\gamma^p; \quad \Delta\gamma^p = (2\Delta e^p_{ij}\Delta e^p_{ji})^{1/2} \tag{9}$$

and h is a hardening modulus:

$$h = \frac{d\mu}{d\gamma^p} \tag{10}$$

EFFECTIVE STRESS ANALYSIS OF SIMPLE SHEAR

As shown in to Figure 1, simple shear of an infinitely long soil layer of thickness $2l$ is considered. The x_1-axis is chosen parallel to the axis of the layer, and it is assumed that all field properties are independent of x_1, varying only in the x_2-direction, i.e. $\partial/\partial x_1 = 0$.

Let S denote a given configuration of the layer. The state of effective stress in the plane of deformation in S is given by

$$(\sigma'_{ij}) = \begin{bmatrix} \sigma'_{11} & \sigma'_{12} \\ \sigma'_{12} & \sigma'_{22} \end{bmatrix} \tag{11}$$

Considering infinitesimal transitions, $S \to S + \Delta S$, emanating from the considered state of initial stress, S, let Δu_1 and Δu_2 denote the incremental displacements of the soil skeleton in the x_1- and x_2-directions, respectively. The non-vanishing components of the corresponding incremental strain tensor are

$$\Delta\varepsilon_{12} = \tfrac{1}{2}\Delta u_{1,2}; \quad \Delta\varepsilon_{22} = \Delta u_{2,2} \tag{12}$$

where

$$(\cdot)_{,i} = \partial/\partial x_i.$$

Undrained simple shear

For undrained homogeneous deformation and incompressible grains and fluid

$$\Delta\varepsilon_{22} = 0 \tag{13}$$

For isotropic initial configurations and monotonous simple shear the constitutive equation (4) shows that throughout the undrained simple shear

$$\sigma'_{11} = \sigma'_{22} = \sigma' \tag{14}$$

and consequently

$$p' = |\sigma'|; \quad \tau = |\sigma_{12}| \tag{15}$$

with

$$\mu = \frac{\tau}{p'} \tag{16}$$

As shown in Figure 2, μ can be identified as

$$\mu = \tan\phi_m \tag{17}$$

where ϕ_m is the so-called mobilized *Coulomb* friction angle. Similarly β can be identified as

$$\beta = \tan\psi_m \tag{18}$$

where ψ_m is called the mobilized dilatancy angle.

For the considered undrained simple-shear motions, the constitutive equation (4) provides a

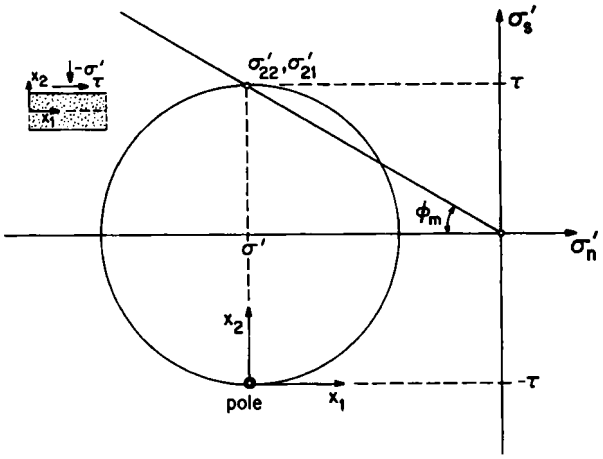

Figure 2. State of stress in undrained simple-shear

simple expression for the tangent modulus, η, to the effective stress-path

$$\eta = \frac{d\tau}{dp'} = -\mu \frac{\chi - \chi_T}{\chi_T} \tag{19}$$

where

$$\chi = \frac{p'}{G} h; \quad \chi_T = -\alpha\mu\beta \tag{20}$$

Figure 3 shows the effective stress-path for contractant material ($\beta < 0$). The state S_T of maximum shear stress is characterized by the condition

$$\chi = \chi_T \tag{21}$$

whereas the state S_C of maximum effective stress obliquity is characterized by the condition

$$\chi = \chi_C = 0 \tag{22}$$

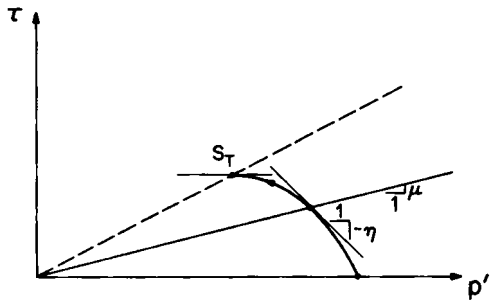

Figure 3. Effective stress path in undrained simple-shear

Drained deformation superimposed on undrained simple shear

In this case the constitutive equation (4) provides the following expressions for the effective stress increments:

$$\begin{bmatrix} \Delta\sigma'_{11} \\ \Delta\sigma'_{22} \\ \Delta\sigma'_{12} \end{bmatrix} = G \begin{bmatrix} \alpha\Lambda_{11} - 2 & -\alpha\Lambda_{12} \\ \alpha\Lambda_{11} & -\alpha\Lambda_{12} \\ -\Lambda_{21} & \Lambda_{22} \end{bmatrix} \begin{bmatrix} \Delta\varepsilon \\ \Delta\gamma \end{bmatrix} \tag{23}$$

where

$$\Delta\varepsilon = \Delta u_{2,2}; \quad \Delta\gamma = \Delta u_{1,2} \tag{24}$$

and

$$(\Lambda_{ij}) = \begin{bmatrix} \dfrac{1+\chi}{1+\chi-\chi_T} + \dfrac{1}{\alpha} & \dfrac{\beta}{1+\chi-\chi_T} \\ \dfrac{\alpha\mu}{1+\chi-\chi_T} & \dfrac{\chi-\chi_T}{1+\chi-\chi_T} \end{bmatrix} \tag{25}$$

STABILITY OF UNDRAINED SHEAR

As explained elsewhere,[8] weak bifurcation solutions can be obtained by means of a perturbation analysis of the trivial undrained deformation. Starting from a state S of initial effective stress, equations (11) and (14), a superimposed undrained simple-shear motion is considered. The resulting deformation mode is a linear combination of a trivial mode and another, yet to be determined inhomogeneous perturbation mode, e.g.

$$\Delta u_i = \Delta\hat{u}_i + \Delta\tilde{u}_i, \quad \text{etc.} \tag{26}$$

The strains caused by the perturbation mode are assumed to be small with respect to the trivial mode ($\| \Delta\tilde{u}_{i,j} \| \ll \| \Delta\hat{u}_{i,j} \|$), in order to ensure the same constitutive description for both the trivial and the non-trivial modes.[8]

Infinitesimal strain and dilatation of the soil skeleton are denoted by $\Delta\varepsilon_{ij}$ and $\Delta\varepsilon$, respectively:

$$\Delta\varepsilon_{ij} = (\Delta u_{i,j} + \Delta u_{j,i})/2; \quad \Delta\varepsilon = \Delta u_{k,k} \tag{27}$$

With $\Delta u_i = \Delta u_i^s$, Δu_i^w, denoting the displacements of the soil skeleton and the pore-water, respectively, the velocities are their time derivatives:

$$\Delta v_i^s = \frac{\partial \Delta u_i^s}{\partial t}; \quad \Delta v_i^w = \frac{\partial \Delta u_j^w}{\partial t} \tag{28}$$

The relative specific discharge vector is then defined as

$$\Delta Q_i = n(\Delta v_i^w - \Delta v_i^s) \tag{29}$$

where n is the porosity.

Field equations

For incompressible grains, mass balances for the solid and aqueous phases are expressed by the following equations:

$$\frac{\Delta n}{1-n} = \Delta\varepsilon \tag{30}$$

$$-\Delta Q_{i,i} = \frac{n}{K_w}\frac{\partial \Delta p}{\partial t} + \frac{\partial \Delta \varepsilon}{\partial t} \tag{31}$$

where K_w is the compressibility of water. Equation (30) simply expresses the fact that for incompressible grains, volume changes are only due to changes in porosity. Equation (31) is the well-known continuity equation.

Balance of linear momentum, on the other hand, is expressed by the conditions

$$\Delta \sigma'_{ij,j} = -\Delta b_i + \rho_1 \frac{\partial^2 \Delta u_i}{\partial t^2} \tag{32}$$

$$-\Delta p_{,i} = \Delta b_i + \rho_2 \frac{\partial^2 \Delta u_i}{\partial t^2} + \rho_w \frac{\partial \Delta Q_i}{\partial t} \tag{33}$$

where ρ_1 and ρ_2 are relative densities

$$\rho_1 = (1-n)\rho_s, \quad \rho_2 = n\rho_w \tag{34}$$

and ρ_s, ρ_w are the densities of the constituents, i.e. of the solid grains and water. In equations (32) and (33) Δb_i is the seepage force that obeys Darcy's law:

$$\Delta b_i = b \Delta Q_i \tag{35}$$

where

$$b = \frac{\rho_w \nu_k}{k} \tag{36}$$

with ν_k being the kinematic viscosity of water and k being the Muskat permeability of the soil skeleton (see Table I).

Table I. Material and system properties for the numerical evaluation of the eigenvalue equations (73) and (82)

Symbol	Value	Description
l[cm]	1	Layer thickness
$\lvert\sigma'\rvert$[kPα]	200	Normal effective stress
ρ_s/ρ_w[−]	2.67	Specific gravity
α[−]	3	$\alpha = K/G = (1-2\nu)^{-1}$
ν_K[cm^2 s^{-1}]	$1{\cdot}002 \times 10^{-2}$	Kinematic viscosity of water (20° C)
e[−]	0·85	Voids ratio
C_S[−]	$1{\cdot}87 \times 10^{-3}$	Swelling index
K[MPa]	198	Compression modulus; $K = \lvert\sigma'\rvert(1+e)/C_S$
k_w[cm s^{-1}]	$4{\cdot}1 \times 10^{-2}$	Permeability for water
k[mm^2]	$4{\cdot}2 \times 10^{-5}$	Muskat permeability; $k = \nu_K k_w/g$
μ[−]	0·577	$\mu = \tan\phi_T$
β[−]	−0·072	$\beta = \tan\psi_T$
χ_T[−]	0·125	equation (20)
ξ[−]	0·5	equation (38)

Governing equations

The constitutive equations (23) together with the balance equations (31)–(33) constitute the set of governing equations. In these equations dimensioned quantities are replaced by the following set of non-dimensional ones:

$$\mathring{x}_i = \frac{x_i}{l}; \quad \mathring{t} = \mathring{\rho}\frac{v_k}{k}t$$

$$\mathring{u}_i = \frac{\Delta\tilde{u}_i}{l}; \quad \mathring{Q}_i = \xi_{(i)}\frac{\Delta\tilde{Q}_i}{c_{(i)}}; \quad \mathring{\rho} = \frac{\Delta\tilde{p}}{K} \tag{37}$$

$$\theta = n\frac{K}{K_w}$$

where

$$\mathring{\rho} = \frac{\rho_1}{\rho_w}$$

$$\xi_2 = \xi; \quad \xi_1 = \xi\sqrt{\alpha}; \quad \xi = \mathring{\rho}\frac{l}{\sqrt{k}}\frac{v_k/\sqrt{k}}{c_2} \tag{38}$$

$$c_2 = (K/\rho_1)^{1/2}; \quad c_1 = (G/\rho_1)^{1/2}$$

In the following the superscript (*) is avoided for simplicity reasons and all appearing quantities are meant to be dimensionless. With the notation $(\cdot)_{,i} = \partial/\partial\mathring{x}_i$ and $(\cdot)_{,t} = \partial/\partial\mathring{t}$, and with $(\cdot)_{,1} = 0$, the governing equations become

$$\Lambda_{11}u_{2,22} - \Lambda_{12}u_{1,22} = -Q_2 + \xi^2 u_{2,tt} \tag{39}$$

$$-\Lambda_{21}u_{2,22} + \Lambda_{22}u_{1,22} = -Q_1 + \alpha\xi^2 u_{1,tt} \tag{40}$$

$$0 = Q_1 + \frac{1}{\rho}(Q_{1,t} + \alpha n\xi^2 u_{1,tt}) \tag{41}$$

$$-p_{,2} = Q_2 + \frac{1}{\rho}(Q_{2,t} + n\xi^2 u_{2,tt}) \tag{42}$$

$$-Q_{2,2} = \xi^2(\theta p_{,t} + u_{2,2t}) \tag{43}$$

The equilibrium in a state S is inherently unstable if solutions for the perturbation mode exist which under appropriate boundary conditions grow exponentially with time. In other words, instability holds if solutions of the form

$$\{u_i, Q_i, p\}^T = e^{ft}\{\hat{u}_i(x_2), \hat{Q}_i(x_2), \hat{p}(x_2)\}^T \tag{44}$$

with positive growth coefficient f exist.

Boundary conditions

Following Figure 1, it is assumed here that the trivial mode satisfies the following non-homogeneous boundary conditions for $x_2 = \pm 1$:

$$\Delta\mathring{\sigma}_{22} = 0; \quad \Delta\mathring{\sigma}_{12} = \Delta\mathring{\tau}; \quad \Delta\mathring{Q}_2 = 0 \tag{45}$$

where $\Delta\mathring{\tau}$, according to equation (19), is negative for states beyond the state $S_T(\chi < \chi_T)$. Assuming

that these boundary conditions also hold for the non-trivial mode, it follows that the perturbation mode satisfies homogeneous boundary conditions for $x_2 = \pm 1$:

$$\Delta\tilde{\sigma}_{22} = \Delta\tilde{\sigma}_{12} = \Delta\tilde{Q}_2 = 0 \tag{46}$$

INERTIA-FREE FORMULATION

Looking at the governing equations (39)–(43) one observes that the acceleration terms for the displacement of the solid are multiplied by the coefficient ξ^2, which according to Table I, is for sand of the order of 10^{-1}. Therefore neglect of inertia terms must be based on an argument that the second partial time derivatives are small quantities. In this case equation (41) provides

$$Q_1 = 0 \tag{47}$$

With the notation of equation (44) and with

$$(\hat{\varepsilon}, \hat{\gamma}) = (\hat{u}_2', \hat{u}_1'); \quad (\cdot)' = \mathrm{d}/\mathrm{d}x_2 \tag{48}$$

the remainder of the governing equations provide

$$\hat{\gamma} = \frac{\Lambda_{21}}{\Lambda_{22}}\hat{\varepsilon} \tag{49}$$

$$\frac{\Lambda}{\Lambda_{22}}\hat{\varepsilon} = \hat{p}; \quad \Lambda = \det(\Lambda_{ij}) = \frac{1+\alpha}{\alpha}\cdot\frac{\chi - \dfrac{1}{1+\alpha}\chi_T}{1+\chi-\chi_T} \tag{50}$$

$$\hat{p}'' = \xi^2 f(\theta\hat{p} + \hat{\varepsilon}) \tag{51}$$

$$\hat{Q}_2 = -\hat{p}' \tag{52}$$

Equations (49) and (50) are a result of the equilibrium and boundary conditions in terms of total stresses. With

$$\hat{\varepsilon} = \varepsilon_0 \cos(m\pi x_2); \quad p = p_0 \cos(m\pi x_2), \quad m = 1, 2, \ldots \tag{53}$$

from equations (49)–(52) it follows that the boundary conditions (46) are identically satisfied. From equations (50) and (51), and for non-trivial solutions in terms of the amplitudes ε_0 and p_0 a condition for the growth coefficient, f, can be derived:

$$f = -\left(\frac{m\pi}{\xi}\right)^2 \frac{1+\alpha}{\alpha}\left(1 - \frac{1+\alpha}{\alpha}\theta\right)\frac{\chi - \dfrac{1}{1+\alpha}\chi_T}{\chi - \chi_{cr}}. \tag{54}$$

where

$$\chi_{cr} = (1-\theta)\chi_T = \chi_T + O(\theta). \tag{55}$$

For incompressible fluid, $\theta = 0$ and $\chi_{cr} = \chi_T$.

Qualitatively similar expressions have been obtained for the growth coefficient from the stability analysis of the undrained plane-strain rectilinear extensions.[8] As already pointed out in the introduction, the expression (54) for the evolution of the growth coefficient is somewhat anomalous, if contractant material ($\chi_{cr} > 0$) is considered. At a state S_{cr}, lying very close to the state S_T of maximum shear stress, the growth coefficient, f, as predicted from an inertia-free formulation, switches from $-\infty$ to $+\infty$. For states following S_{cr}, f evolves as $(\chi - \chi_{cr})^{-1}$, i.e. continuously decreasing, which contradicts the experimental evidence.[3]

As equation (54) demonstrates, this anomalous evolution law for f is not restored by considering

compressibility of the fluid, which produces a more or less insignificant shift of the instability point away from S_T to states of higher stress obliquity.

It should be emphasized that consideration of large strains[8] does not alter the singular character of the solution. In this case, and for incompressible fluid, the corresponding expression for the growth coefficient becomes:

$$f = -\left(\frac{m\pi}{\xi^2}\right)\frac{1+\alpha}{\alpha}\cdot\frac{\chi - \dfrac{1}{1+\alpha}\chi_T - \chi'}{\chi - \chi_T} \tag{56}$$

where

$$\chi' = \frac{\alpha}{1+\alpha}(1+\chi-\chi_T)\mu\frac{\tau}{G}\left(\frac{\tau}{G} \ll 1\right) \tag{57}$$

These observations motivated the consideration of the fully dynamical set of equations (39)–(43) in order to investigate the question of the above presented anomaly in the evolution of the growth coefficient and with that the credibility of the analysis can be restored. This analysis is given in the following sections.

DYNAMIC STABILITY ANALYSIS

Equation (41), expressing the balance of linear momentum for the fluid in the x_1-direction, can be used to prove that the relative specific discharge in this direction, ΔQ_1, is negligible:

$$\hat{Q}_1 = -\hat{u}_1\frac{\alpha n\xi^2}{\rho+f}f^2 \quad \text{or} \quad \hat{Q}_1 = O(f^2) \tag{58}$$

The remainder of the governing equations (39)–(43) can be uncoupled, and the various field properties can be expressed in terms of the dilatation $\hat{\varepsilon}$:

$$\hat{\gamma} = \frac{1}{\Lambda_{12}}(\lambda^{-2}\hat{\varepsilon}'' - \kappa\Lambda_{22}\hat{\varepsilon}) \tag{59}$$

$$\hat{p}'' = f\xi^2\left(1+\frac{f\rho}{1-n}\right)\hat{\varepsilon} \tag{60}$$

$$\hat{Q}_2' = -f\xi^2\hat{\varepsilon} \tag{61}$$

where

$$\lambda = f\xi\sqrt{\left(\frac{\alpha}{\Lambda}\right)}; \quad \kappa = \alpha\frac{1+f}{f} \tag{62}$$

The dilatation $\hat{\varepsilon}$ is then the solution of the following differential equation:

$$\hat{\varepsilon}^{(iv)} - \lambda^2 A\hat{\varepsilon}'' + \lambda^4 B\hat{\varepsilon} = 0 \tag{63}$$

where

$$A = \kappa\Lambda_{22} + \Lambda_{11}; \quad B = \kappa\Lambda \tag{64}$$

For

$$\hat{\varepsilon} = \varepsilon_0 \exp(\lambda\Gamma x_2) \tag{65}$$

Γ is given by the following characteristic equation:

$$\Gamma^4 - A\Gamma^2 + B = 0 \tag{66}$$

The number of integration constants can be reduced if the following symmetry conditions are

considered:

$$\hat{t}(x_2) = \hat{t}(-x_2) \Rightarrow \hat{\varepsilon}(x_2) = \hat{\varepsilon}(-x_2) \tag{67}$$

$$\hat{Q}_2(0) = 0 \Rightarrow \hat{Q}_2 = -f\xi^2 \int \hat{\varepsilon} \tag{68}$$

$$\hat{u}_2(0) = 0 \Rightarrow \hat{p} = C_3 + f\xi^2 \left(1 + \frac{f\rho}{1-n}\right) \iint \hat{\varepsilon} \tag{69}$$

Using the above expressions (59)–(61) and symmetry conditions (67)–(69) for the various fields, the boundary conditions (46) provide a (3 × 3) homogeneous algebraic system with respect to the two integration constants C_1 and C_2 for the dilatation $\hat{\varepsilon}$ and the integration constant C_3 for the pressure $\hat{p}$, equation (69). For non-trivial solutions of this system, eigenvalue equations can be derived from the condition that the system determinant must be zero.

EIGENVALUE EQUATIONS

The type of the governing differential equation (63) depends on the type of the roots of the characteristic equation (66). Let

$$D = A^2 - 4B \tag{70}$$

be the discriminant of equation (66). The solutions and the corresponding eigenvalue equations in the various characteristic regimes are given below.

EC (elliptic complex): $B > 0$ $(\Lambda > 0)$, $D < 0$

$$\begin{aligned} &\Gamma_{1/2} = \pm w; \quad \Gamma_{3/4} = \pm \bar{w}; \quad w = M + \mathrm{i}N, \quad \mathrm{i} = \sqrt{(-1)}, \\ &M = [(\sqrt{B} + A/2)/2]^{1/2}; \quad N = [(\sqrt{B} - A/2)/2]^{1/2} \end{aligned} \tag{71}$$

$$\hat{\varepsilon} = C_1 \cosh(\lambda M x_2)\cos(\lambda N x_2) + C_2 \sinh(\lambda M x_2)\sin(\lambda N x_2) \tag{72}$$

The eigenvalue equation in the EC regime becomes

$$\frac{\sin(2\lambda N)}{\sinh(2\lambda M)} = \frac{N\Lambda + \Lambda_{22}\sqrt{B}}{M\Lambda - \Lambda_{22}\sqrt{B}} \tag{73}$$

EI (elliptic imaginary): $A < 0$, $B > 0$ $(\Lambda > 0)$, $D > 0$

$$\begin{aligned} &\Gamma_{1/2} = \pm \mathrm{i}w_1; \quad \Gamma_{3/4} = \pm \mathrm{i}w_2, \quad \mathrm{i} = \sqrt{-1} \\ &w_{1/2} = [(-A \mp \sqrt{D})/2]^{1/2} \end{aligned} \tag{74}$$

$$\hat{\varepsilon} = C_1 \cos(\lambda w_1 x_2) + C_2 \cos(\lambda w_2 x_2) \tag{75}$$

The eigenvalue equation in the EI regime becomes

$$\frac{\tan(\lambda w_1)}{\tan(\lambda w_2)} = \frac{w_1}{w_2} \frac{\Lambda_{22}(w_1^2 + \kappa\Lambda_{22}) + \Lambda_{12}\Lambda_{21}}{\Lambda_{22}(w_2^2 + \kappa\Lambda_{22}) + \Lambda_{12}\Lambda_{21}} \tag{76}$$

P (parabolic): $B < 0$ $(\Lambda < 0;\ D > 0,\ |A| > \sqrt{D})$

$$\begin{aligned} &\Gamma_{1/2} = \pm w_1; \quad \Gamma_{3/4} = \pm \mathrm{i}w_2, \quad \mathrm{i} = \sqrt{-1} \\ &w_{1/2} = [(\mp A + \sqrt{D})/2]^{1/2} \end{aligned} \tag{77}$$

$$\hat{\varepsilon} = C_1 \cosh(\lambda w_1 x_2) + C_2 \cos(\lambda w_2 x_2) \tag{78}$$

where $\lambda = \xi f \sqrt{\alpha} / \sqrt{|\Lambda|}$. The eigenvalue equation in the P regime becomes

$$\frac{\tanh(\lambda w_1)}{\tan(\lambda w_2)} = \frac{w_1}{w_2} \frac{\Lambda_{22}(w_1^2 + \kappa\Lambda_{22}) + \Lambda_{12}\Lambda_{21}}{\Lambda_{22}(-w_2^2 + \kappa\Lambda_{22}) + \Lambda_{12}\Lambda_{21}} \tag{79}$$

H (hyperbolic): $A > 0$, $B > 0$ ($\Lambda > 0$), $D > 0$

$$\Gamma_{1/2} = \pm w_1; \quad \Gamma_{3/4} = \pm w_2$$
$$w_{1/2} = [(A \pm \sqrt{D})/2]^{1/2} \tag{80}$$

$$\hat{\varepsilon} = C_1 \cosh(\lambda w_1 x_2) + C_2 \cosh(\lambda w_2 x_2). \tag{81}$$

And, finally, the eigenvalue equation in the H regime becomes:

$$\frac{\tanh(\lambda w_1)}{\tanh(\lambda w_2)} = \frac{w_1}{w_2} \frac{\Lambda_{22}(w_1^2 - \kappa\Lambda_{22}) - \Lambda_{12}\Lambda_{21}}{\Lambda_{22}(w_2^2 - \kappa\Lambda_{22}) - \Lambda_{12}\Lambda_{21}} \tag{82}$$

COMPUTATIONAL RESULTS AND ASYMPTOTIC FORMULAE

Among the solution of the eigenvalue equations, listed above, we distinguish here between those holding in the hardening regime ($\chi > 0$) and those holding in the softening regime ($\chi < 0$) of the background drained behaviour.

Solutions in the hardening regime

The only solutions found in the hardening regime are those holding for contractant material ($\beta < 0$) and for states subsequent to the state S_T of maximum shear stress. States lying in the immediate vicinity of S_T (i.e. states with $0 < -(\chi - \chi_T) \ll 1$) are in the EC regime of the governing differential equation (63). States more distant from S_T and closer to S_C are in the H regime of equation (63). To demonstrate this, the corresponding eigenvalue equations (73) and (82) have been solved numerically and for a set of material properties that are typical for a loose sand layer. Table I summarizes the assumed material and system properties. The layer thickness and the effective stress level correspond to values that are typical for laboratory conditions. Figure 4 shows the

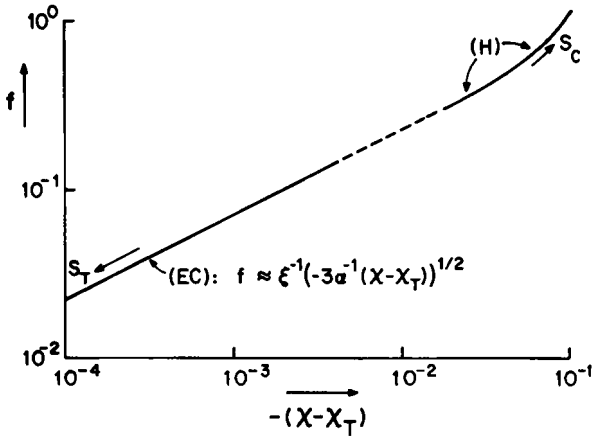

Figure 4. Eigensolution in the hardening regime of a contractant soil layer (Table I)

computational result. The initial branch of the obtained curve describing the solution in the immediate vicinity of S_T, is given by the following asymptotic solution of equation (73):

$$f = \xi^{-1}\left[-\frac{3}{\alpha}(\chi - \chi_T)\right]^{1/2} \tag{83}$$

This formula demonstrates the finding that for contractant material any state beyond the state S_T is inherently unstable; the instability evolves as e^{ft}, with the exponent f proportional to $|\chi - \chi_T|^{1/2}$. This demonstrates the catastrophic nature of liquefaction phenomena, since the instability evolves at S_T at an infinite pace.

Solutions in the softening regime

The only physically meaningful solutions found in the softening regime are those holding for dilatant material ($\beta > 0$) and for states subsequent to a state S'_C which is after the state S_C and before the state S_T. S'_C is characterized by the condition:

$$\chi = \chi'_C = \frac{1}{1+\alpha}\chi_T \tag{84}$$

All these unstable states are in the P-regime of equation (63). In the vicinity of S'_C, infinitely many branches of the solution exist, since for small $|\chi - \chi'_C|$-values equation (79) reduces to the following.

$$\tan\sqrt{w} = 0 \tag{85}$$

where

$$w = \xi^2 f \frac{\Lambda_{22}}{|\Lambda|} \tag{86}$$

Equation (85) is satisfied by the solution, $\sqrt{w} = m\pi$ ($m = 1, 2, \ldots$), or by

$$f = \left(\frac{m\pi}{\xi}\right)^2 \frac{|\chi - \chi'_C|}{\chi - \chi_T} \tag{87}$$

This formula demonstrates the fact that for dilatant material, states beyond the state S'_C are inherently unstable; see also equations (54) and (56). This observation modifies slightly the findings by Rice[5], who studied the stability of dilatant hardening by using a simplified version of the elastoplastic constitutive law for pressure-sensitive, dilatant material. In this analysis, instability occurs immediately after the state S_C of maximum effective stress obliquity.

CONCLUDING REMARKS

The present stability analysis of undrained simple shear has demonstrated that, in terms of effective stresses, liquefaction is not strictly a material property but an instability phenomenon of a soil-skeleton–water system subjected to dead loading boundary conditions, the system itself being defined by a set of constitutive equations, its geometry and its initial state of stress. The derived evolution law of the growth coefficient for the instability at S_T, equation (83), is describing only the initial phase of the post-failure deformation, usually termed as flow deformation.

The present findings should be of importance to someone who is interested in numerically simulating the flow deformation of a liquefying solid body. If this is to be pursued, the analysis has shown that among the various factors which may influence the result, such as fluid compressibility,

large strains or inertial effects, only the latter is significant. In other words, numerical studies of liquefaction phenomena should be performed by using a dynamic formulation. In addition, one should keep in mind that in the regime of flow deformation the governing differential equations change type rapidly or, as in the inertia-free formulation, yield to improperly posed mathematical problems.[9] As was demonstrated recently by Sandler and Wright[10] in the case of an ill-posed boundary value with strain-softening, severe numerical problems do arise which are at present not satisfactorily answered. In general, the techniques needed to trace the evolution of solutions in the 'post-failure' regime consist of appropriate perturbations of the fully non-linear governing equations and consideration of physical effects (such as rate sensitivity or inertial effects) which may become significant under these conditions.

ACKNOWLEDGEMENT

The author wants to thank Professor H. Winter of the Fachhochschule Stuttgart for his valuable suggestions and the U.S. National Science Foundation for supporting this research through Grant CEE-8216418.

REFERENCES

1. A. Casagrande, 'Liquefaction and cyclic deformation of sands. A critical review', *Harvard Soil Mechanics Series No. 88*, 1976.
2. G. Castro, 'Liquefaction of sands', *Ph.D. Thesis*, Harvard University, *Harvard Soil Mechanics Series No. 81*, 1969.
3. Y. P. Vaid and J. C. Chern, 'Effect of static shear on resistance to liquefaction', *Soils and Foundations*, **23**, 47–60 (1983).
4. G. Gudehus, F. Darve and I. Vardoulakis (eds). *Constitutive Relations for Soils*, A. A. Balkema, 1984.
5. J. R. Rice, 'On the stability of dilatant hardening for saturated rock masses', *J. Geoph. Res.*, **80**, 1531–1536 (1976).
6. J. Mandel, 'Conditions de stabilite et postulat de Drucker', *IUTAM Symposium on Rheology and Soil Mechanics*, Springer-Verlag, 1966, pp. 58–67.
7. Z. Mroz, 'Non-associate flow laws in plasticity', *Journal de Mechanique*, **2**, (1963).
8. I. Vardoulakis, 'Stability and bifurcation of undrained plane rectilinear deformations on water-saturated granular soils', *Int. j. numer. anal. methods geomech*, **9**, 399–414 (1985).
9. L. E. Payne, 'Improperly posed problems in partial differential equations', *SIAM Publ., Regional Conf. Series in Appl. Math.*, (1976).
10. I. S. Sandler and J. P. Wright, 'Strain-softening', in *Mechanics of Inelastic Solids 6, Proc. of the Workshop on Theoretical Foundation for Large-Scale Computations of Non-Linear Material Behavior*, 1984, Chapt. XI, pp. 285–296.